

# Preparation of Yellow Core–Blue Shell Coordination Polymer Nanoparticles Using Active Surface Coordination Sites on a Prussian-blue Analog

Manabu Ishizaki,<sup>1</sup> Yoshie Sajima,<sup>1</sup> Shoko Tsuruta,<sup>1</sup> Akihito Gotoh,<sup>1</sup> Masatomi Sakamoto,<sup>1,2</sup>  
Tohru Kawamoto,<sup>2</sup> Hisashi Tanaka,<sup>2</sup> and Masato Kurihara<sup>\*1,2</sup>

<sup>1</sup>Department of Material and Biological Chemistry, Faculty of Science, Yamagata University,  
1-4-12 Kojirakawa-machi, Yamagata 990-8560

<sup>2</sup>Nanotechnology Research Institute, National Institute of Advanced Industrial Science and Technology (AIST),  
1-1-1 Umezono, Tsukuba 305-8568

(Received August 18, 2009; CL-090758; E-mail: kurihara@sci.kj.yamagata-u.ac.jp)

Yellow core–blue shell coordination polymer nanoparticles were prepared through the combination of  $\text{Fe}^{2+}$  to the surface  $\text{Fe}^{\text{III}}\text{--CN}$  sites exposed on the yellow core nanoparticles of nickel hexacyanoferrate,  $\text{K}_{0.12}\text{Ni}_{3.0}[\text{Fe}(\text{CN})_6]_{2.04} \cdot 14\text{H}_2\text{O}$ . The  $\text{Fe}^{2+}$ -attached surface shell layer,  $\text{Fe}^{\text{II}}\text{--NC--Fe}^{\text{III}}$ , changed into the Prussian blue-like valence state,  $\text{Fe}^{\text{III}}\text{--NC--Fe}^{\text{II}}$ , via single-electron transfer.

Prussian blue (PB) pigment, with its three-century history, is recognized as the first synthetic coordination polymer.<sup>1</sup> The multifunctionalities of PB and its analogs (PBAs) have recently renewed scientific as well as industrial applications,<sup>2</sup> such as electrochromic displays,<sup>3</sup> electrocatalysts,<sup>4</sup> fuel cell electrodes,<sup>5</sup> secondary batteries,<sup>6</sup> ion- and biosensors,<sup>7</sup> photomagnets,<sup>8</sup> and hydrogen storage.<sup>9</sup> In common syntheses,  $\text{M}^{3+/2+}$  and  $[\text{Fe}^{\text{II/III}}(\text{CN})_6]^{4-/3-}$  are reacted in an aqueous solution, and the as-formed PB and PBAs are initially suspended as colloidal particles but immediately precipitated as an insoluble solid. Various attempts have been made in the last decade to provide PB and PBA nanoparticles and their dispersion solution by reversed micelle,<sup>10</sup> polymer protection,<sup>11</sup> and template<sup>12</sup> techniques. In 2007, we showed a renewed understanding that the PB, nickel hexacyanoferrate (Ni–PBA), and cobalt hexacyanoferrate (Co–PBA) insoluble solids were a physically aggregated form of 10–20-nm nanoparticles,<sup>13</sup> i.e., historically so-called “colloidal particles,” from their consistency between Scherrer’s and transmission electron microscope sizes. Based on the insoluble PB and PBAs as nanoparticles, we have focused on their active surface coordination sites, where the three-dimensional cyano-bridged coordination bonding of  $\text{Fe--CN--M}$  is discontinued and two types of active coordination sites,  $\text{Fe--CN}$  and  $\text{M--H}_2\text{O}$ , are exposed on the surface (Figure 1a). Through surface modification with alkylamines and  $[\text{Fe}^{\text{II}}(\text{CN})_6]^{4-}$  using the surface  $\text{Fe}^{\text{III}}\text{--H}_2\text{O}$  sites, we achieved the simple transformation of the PB-insoluble solid into toluene- and water-dispersible nanoparticles, respectively.<sup>13</sup> In an ideal PB nanocube, the 10-nm nanocubes bear 15% surface  $\text{Fe}^{\text{III}}\text{--H}_2\text{O}$  sites, numerically, of all Fe ions.<sup>14</sup> The surface coverage was experimentally saturated by ca. 15% surface modification using  $[\text{Fe}^{\text{II}}(\text{CN})_6]^{4-}$ .

In this study, we will propose a pioneering nanoarchitecture using such surface coordination space on the coordination polymer nanoparticles. In the first attempt, we adopted the formation of the surface PB-like layer of  $\text{Fe--CN--Fe}$  on Ni–PBA yellow nanoparticles, in which  $\text{Fe}^{\text{II}}$  ions could be combined with the  $\text{Fe}^{\text{III}}\text{--CN}$  sites exposed on the surface (Figure 1b).

Ni–PBA was isolated as a yellow insoluble nanoparticle solid of  $\text{K}_{0.12}\text{Ni}_{3.0}[\text{Fe}(\text{CN})_6]_{2.04} \cdot 14\text{H}_2\text{O}$  from a dense aqueous mix-

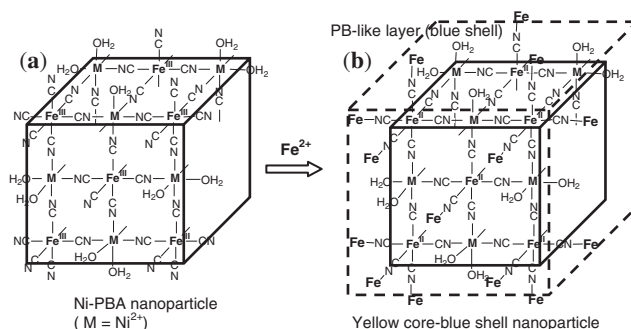


**Figure 1.** Synthetic strategy of yellow core–blue shell nanoparticles from the insoluble Ni–PBA nanoparticle solid via the surface modification with  $\text{Fe}^{2+}$  to  $\text{Fe}^{\text{III}}\text{--CN}$  sites. The Ni–PBA nanoparticles are drawn as an ideal cubic shape (nanocube) surrounded by six {100} surfaces and consisting of a 3 × 3 metal arrangement with a 0.5 nm × 2 dimension.

ture of  $\text{Ni}(\text{NO}_3)_2 \cdot 6\text{H}_2\text{O}$  and  $\text{K}_3[\text{Fe}(\text{CN})_6]$ , according to the literature,<sup>13</sup> where the metal composition and hydration number were determined by wavelength-dispersive X-ray spectroscopy (WDX) and thermogravimetric analyses, respectively. As already reported, the Scherrer’s particle size of the insoluble Ni–PBA is estimated as 11.6 nm from the line broadening of powder X-ray diffraction (XRD) signals (Figure 1a). The surface modification with  $\text{Fe}^{2+}$  to  $\text{Fe}^{\text{III}}\text{--CN}$  sites was investigated on the addition number of  $\text{FeSO}_4$  between 1 and 40% to Ni–PBA, numerically, of all transition-metal ions of Fe and Ni.<sup>14</sup> Into an aqueous suspension (4 mL) of Ni–PBA (1.00 g,  $1.17 \times 10^{-3}$  mol), an aqueous solution (3 mL) of  $\text{FeSO}_4 \cdot 7\text{H}_2\text{O}$  (16.2–648 mg,  $5.83 \times 10^{-5}$ – $2.33 \times 10^{-3}$  mol) was added and stirred for 1 day. After centrifugation at 15000 rpm (22140 G), the sediment was washed with water six times to carefully remove unreacted  $\text{FeSO}_4$  and then dried under reduced pressure. The powdery solids exhibited color gradation from yellow to green depending on the addition number of  $\text{Fe}^{2+}$ . The XRD patterns of the solids were unaltered after the reaction with  $\text{Fe}^{2+}$ , indicating that no significant change of the crystal structure or size (11.3 nm) occurred (Figure S1b).<sup>15</sup> The metal ratios of Fe/Ni (mole/mole) of the yellow-to-green solids were estimated from the WDX analyses (Figure 2). The Fe content corresponds to the addition numbers of  $\text{FeSO}_4$  between 1 and 15% and deviates from them above 15%. The Fe/Ni ratios are almost independent of an addition number of more than 15%, but there is a gradual increase of the ratio. The initial yellow color of Ni–PBA changed to green up to addition numbers of 15%, but the green color was visually maintained with the addition of more than 15%. These facts suggest the limited sites of the insoluble Ni–PBA solid to bind  $\text{Fe}^{2+}$  in number, which is ca. 15%. When the insoluble Ni–PBA is a

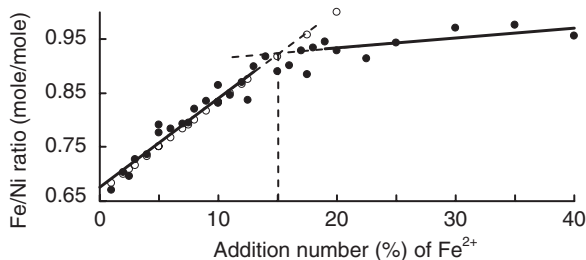


**Figure 2.** Metal ratios (solid circles) of Fe/Ni (mole/mole) of the yellow core–blue shell nanoparticles estimated by the WDX analyses. Open circles show the case in which all of  $\text{Fe}^{2+}$  is chemisorbed on Ni–PBA.

physically aggregated nanoparticle solid of 10-nm Scherrer's size, each nanoparticle bears the surface  $\text{Fe}^{\text{III}}$ –CN sites occupying 15%, numerically, of all transition-metal ions as an ideal nanocube (Figure 1a).<sup>13,14</sup> The experimentally valid number is consistent with that of the size-dependent surface Fe–CN sites on the individual 10-nm Ni–PBA nanoparticles. In a possible reaction mechanism to afford the greenish solids, the surface  $\text{Fe}^{\text{III}}$ –CN sites of Ni–PBA predominantly capture  $\text{Fe}^{2+}$ , but the surface  $\text{Ni}^{2+}$  ions may be partially displaced with  $\text{Fe}^{2+}$  based on the gradual increase in the Fe/Ni ratio on more than a 15% addition. In the FT-IR spectrum, a new absorption band at  $2063\text{ cm}^{-1}$  beside the CN stretching bands at  $2097$  and  $2166\text{ cm}^{-1}$  of Ni–PBA appears and intensifies as the addition number of  $\text{Fe}^{2+}$  increases (Figure 3a). According to the consistency of the new band with that of insoluble PB at  $2063\text{ cm}^{-1}$ , the  $\text{Fe}^{2+}$ -attached surface layer,  $\text{Fe}^{\text{II}}$ –NC– $\text{Fe}^{\text{III}}$ , changes into PB-like valence state,  $\text{Fe}^{\text{III}}$ –NC– $\text{Fe}^{\text{II}}$ , via single-electron transfer to generate yellow core–blue shell coordination polymer nanoparticles, whose color visually depends on the coverage of the PB-like layer.

In the second attempt to fabricate water-dispersible nanoparticles, the surface modification of  $[\text{Fe}^{\text{II}}(\text{CN})_6]^{4-}$  was performed via the ligand exchange of the surface  $\text{Ni}^{\text{II}}$ – $\text{OH}_2$  sites of the initial Ni–PBA and/or  $\text{Fe}^{\text{III}}$ – $\text{OH}_2$  sites of the PB-like layer of the yellow core–blue shell PBA nanoparticles to produce the charged surface layer,  $\text{Ni}^{\text{II}}$ – $[\text{NC}-\text{Fe}^{\text{II}}(\text{CN})_5]^{4-}$  and/or  $\text{Fe}^{\text{III}}$ – $[\text{NC}-\text{Fe}^{\text{II}}(\text{CN})_5]^{4-}$  (Figure S2).<sup>15</sup> According to a previous report of surface-charged water-dispersible PB nanoparticles,<sup>13</sup> the core–shell PBA nanoparticle solids (0.20 g) were stirred for 3 days in water (2 mL) with  $\text{Na}_4[\text{Fe}(\text{CN})_6] \cdot 10\text{H}_2\text{O}$  (30%, numerically, of all transition-metal ions). After centrifugation at 15000 rpm (22140 G) to remove unreacted  $\text{Na}_4[\text{Fe}(\text{CN})_6]$ , the sediment was stirred with water and almost dispersed into water in the same way as the core–shell PBA nanoparticles to exhibit yellow-to-green color with high transparency (Figure S3)<sup>15</sup> on the basis of the UV–vis–near IR absorption spectra (Figure 3b). The absorption band ( $\lambda_{\text{max}} = 767\text{ nm}$ ) is ascribable to the charge-transfer band of the PB-like layer, based on a similar absorption band due to the mixed-valence state of  $\text{Fe}^{\text{II}}$ –CN– $\text{Fe}^{\text{III}}$  at around 700 nm of the water-dispersible PB nanoparticles,<sup>13</sup> and intensifies as the coverage of the PB-like layer increases (Figure 3b). In the typical dispersion solution at 15% coverage, the number-averaged dynamic light-scattering (DLS) particle size is  $22 \pm 4\text{ nm}$  in a high-concentration dispersion solution ( $0.1\text{ g mL}^{-1}$ ) (Figure S4),<sup>15</sup> and the zeta potential of the nanoparticles is  $-26\text{ mV}$  in the dilute dispersion solution. The core–shell PBA nanoparticles are stably dispersed in water through electrostatic repulsion of the surface negative charges. The water-dis-

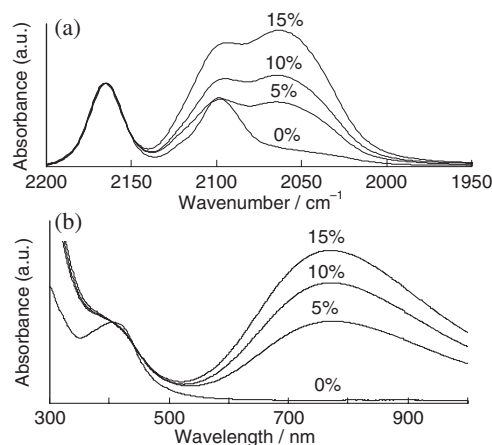


**Figure 3.** FT-IR (a) and UV–vis–near IR absorption spectra (b) of the yellow core–blue shell nanoparticles. The absorption intensity is normalized by that of Ni–PBA.

persible core–shell PBA nanoparticles were observed as the averaged diameter of 9.1 nm on a mica substrate from the atomic force microscopy (AFM) images (Figure S5).<sup>15</sup>

In conclusion, we have developed surface nanoarchitecture of coordination polymer nanoparticles using their specific unsaturated surface coordination sites. The surface  $\text{Fe}^{\text{III}}$ –CN site chemisorbs  $\text{Fe}^{2+}$  on Ni–PBA, and the as-formed  $\text{Fe}^{\text{III}}$ –CN– $\text{Fe}^{\text{II}}$  layer changes into the PB-like valence state,  $\text{Fe}^{\text{II}}$ –CN– $\text{Fe}^{\text{III}}$ , via single-electron transfer to generate yellow core–blue shell coordination polymer nanoparticles.

This work was supported by a Grant-in-Aid for Scientific Research (C) (No. 21550055) of the Japan Society for the Promotion of Science (JSPS) and the Industrial Technology Research Grant Program (No. 06A22203a) in FY2006 from the New Energy and Industrial Technology Development Organization (NEDO) of Japan.

#### References and Notes

- 1 A. Kraft, *Bull. Hist. Chem.* **2008**, *33*, 61.
- 2 M. Kurihara, *Bull. Jpn. Soc. Coord. Chem.* **2007**, *49*, 34.
- 3 S. Hara, H. Shiozaki, A. Omura, H. Tanaka, T. Kawamoto, M. Tokumoto, M. Yamada, A. Gotoh, M. Kurihara, M. Sakamoto, *Appl. Phys. Express* **2008**, *1*, 104002.
- 4 K. Itaya, N. Shoji, I. Uchida, *J. Am. Chem. Soc.* **1984**, *106*, 3423.
- 5 G. Selvarani, S. K. Prashant, A. K. Sahu, P. Sridhar, S. Pitchhuman, A. K. Shukla, *J. Power Sources* **2008**, *178*, 86.
- 6 A. Eftekhari, *J. Power Sources* **2004**, *132*, 291.
- 7 M. Yang, J. Jiang, Y. Yang, X. Chen, G. Shen, R. Yu, *Biosens. Bioelectron.* **2006**, *21*, 1791.
- 8 O. Sato, S. Hayami, Y. Einaga, Z. Z. Gu, *Bull. Chem. Soc. Jpn.* **2003**, *76*, 443.
- 9 S. S. Kaye, J. R. Long, *J. Am. Chem. Soc.* **2005**, *127*, 6506.
- 10 S. Vaucher, M. Li, S. Mann, *Angew. Chem., Int. Ed.* **2000**, *39*, 1793.
- 11 T. Uemura, M. Ohba, S. Kitagawa, *Inorg. Chem.* **2004**, *43*, 7339.
- 12 J. M. Domínguez-Vera, E. Colacio, *Inorg. Chem.* **2003**, *42*, 6983.
- 13 A. Gotoh, H. Uchida, M. Ishizaki, T. Satoh, S. Kaga, S. Okamoto, M. Ohta, M. Sakamoto, T. Kawamoto, H. Tanaka, M. Tokumoto, S. Hara, H. Shiozaki, M. Yamada, M. Miyake, M. Kurihara, *Nanotechnology* **2007**, *18*, 345609.
- 14 The nanoparticles bear size-dependent surface metals whose number is defined by  $[(\text{number of surface metal atoms})/(\text{number of total metal atoms of each nanoparticle}) \times 100 (\%) ]$ .
- 15 Supporting Information is available electronically on the CSJ-Journal Web site, <http://www.csj.jp/journals/chem-lett/index.html>.